Published in final edited form as:
Brain Behav Immun. 2013 February ; 28: . doi:10.1016/j.bbi.2012.07.013.

Restraint stress alters neutrophil and macrophage phenotypes during wound healing

Stéphanie D. Tymen[a], **Isolde G. Rojas**[b], **Xiaofeng Zhou**[a,c], **Zong Juan Fang**[a], **Yan Zhao**[a], and **Phillip T. Marucha**[a,*]

[a]Department of Periodontics, Center for Wound Healing and Tissue Regeneration, College of Dentistry, University of Illinois at Chicago, Chicago, IL, USA

[b]Department of Oral Surgery and Laboratory of Oral Biology and Pathology, College of Dentistry, University of Concepción, Concepción, Chile

[c]Center for Molecular Biology of Oral Diseases, College of Dentistry, University of Illinois at Chicago, Chicago, IL 60612, USA

Abstract

Previous studies reported that stress delays wound healing, impairs bacterial clearance, and elevates the risk for opportunistic infection. Neutrophils and macrophages are responsible for the removal of bacteria present at the wound site. The appropriate recruitment and functions of these cells are necessary for efficient bacterial clearance. In our current study we found that restraint stress induced an excessive recruitment of neutrophils extending the inflammatory phase of healing, and the gene expression of neutrophil attracting chemokines MIP-2 and KC. However, restraint stress did not affect macrophage infiltration. Stress decreased the phagocytic abilities of phagocytic cells *ex vivo*, yet it did not affect superoxide production. The cell surface expression of adhesion molecules CD11b and TLR4 were decreased in peripheral blood monocytes in stressed mice. The phenotype of macrophages present at the wound site was also altered. Gene expression of markers of pro-inflammatory classically activated macrophages, CXCL10 and CCL5, were down-regulated; as were markers associated with wound healing macrophages, CCL22, IGF-1, RELMα; and the regulatory macrophage marker, chemokine CCL1. Restraint stress also induced up-regulation of IL10 gene expression. In summary, our study has shown that restraint stress suppresses the phenotype shift of the macrophage population, as compared to the changes observed during normal wound healing, while the number of macrophages remains constant. We also observed a general suppression of chemokine gene expression. Modulation of the macrophage phenotype could provide a new therapeutic approach in the treatment of wounds under stress conditions in the clinical setting.

Keywords

Restraint stress; Wound healing; Neutrophil; Chemokine; Phagocytosis; Macrophage activation

*Corresponding author. Address: Department of Periodontics, Center for Wound Healing and Tissue Regeneration, University of Illinois at Chicago, 801 S. Paulina Street, Chicago, IL 60612, USA. Tel: +1 312 996 7515; fax: +1 312 996 0943. marucha@uic.edu, stymen2@uic.edu (P.T. Marucha).

1. Introduction

Wound healing requires the timely orchestration and efficient execution of three major overlapping phases: inflammation, proliferation and resolution/remodeling. These phases prevent bacterial infection, repair the damaged tissue and restore tissue function.

Unfortunately many factors, including stress, can hinder a successful outcome. Stress delays wound healing and impairs bacterial clearance (Padgett et al., 1998; Mercado et al., 2002; Rojas et al., 2002; Horan et al., 2005; Eijkelkamp et al., 2007; Williams et al., 2012). Whether the wound is caused by an accident or a surgical procedure, inefficient removal of bacteria at the site of an injury elevates the risk for opportunistic infection. Infection can potentially prolong discomfort to the patient, increase the cost of wound treatment and extend the hospital stay. Neutrophils and macrophages are innate immune system cells responsible for bacterial clearance at the wound. Previous studies have shown that the appropriate recruitment and functions of these cells are crucial for efficient removal of microbial agents (Bullard et al., 1996; Savill, 1997).

After injury, neutrophils and macrophages leave the peripheral blood to reach the wound. Adhesion molecules on the cell surface (e.g. CD11b) facilitate their migration toward a gradient of chemoattractant leading to the inflammatory site. Neutrophils arrive following a trail of chemokines KC and MIP-2 (Engelhardt et al., 1998; Kernacki et al., 2000; Wetzler et al., 2000). Macrophages recruited by MIP-1α and MCP-1, reach the wound shortly after (DiPietro et al., 1998; Maus et al., 2001). At the wound site, neutrophils and macrophages clear bacteria using oxidative burst and phagocytosis. The phenotype and function of the macrophages vary depending on how they are activated. Pathogen recognition as well as the cytokines and chemokines in the environment shape macrophage activation. Activated macrophages can be classified in three groups: classically activated macrophages (CAM), wound-healing macrophages (WHM) and regulatory macrophages (Edwards et al., 2006; Mosser and Edwards, 2008). Each sub-population exhibits specific markers and functions. Classically activated macrophages (CAM) are induced by recognition of microbial patterns via Toll-like receptors (TLR) (Padgett et al., 1998) and cytokines. These pro-inflammatory macrophages express CXCL10 and efficiently kill pathogens (Martinez et al., 2008). Wound-healing macrophages (WHM) arise in response to interleukin-4 (IL-4) and are less proficient than CAM to clear bacteria. However, WHM secrete components of the extracellular matrix and express numerous markers of tissue-remodeling, such as Resistin Like Molecule Alpha (RELMα) and Insulin Growth Factor 1 (IGF-1), which are important during the proliferation and remodeling phases of wound healing. WHM also limit the inflammatory response (Rodero and Khosrotehrani, 2010). Finally, regulatory macrophages also show anti-inflammatory properties, which help in the resolution of inflammation. These cells express CCL1 and IL-10, a potent anti-inflammatory cytokine (Sironi et al., 2006). The macrophage phenotype is not static; macrophages retain their plasticity and are responsive to their environment, which allows them to adapt their phenotype and gene expression profile as wound healing progresses (Daley et al., 2010; Rodero and Khosrotehrani, 2010).

Given the crucial role of neutrophils and macrophages in the removal of bacteria, any factors altering their recruitment and function could impair bacterial clearance. Previous reports have shown that stress modulates neutrophil and macrophage recruitment, chemokine gene expression and the adhesion molecule expression (Curry et al., 2010; Filep et al., 1997; Heasman et al., 2003; Mizobe et al., 1997; Viswanathan and Dhabhar, 2005; Zhang et al., 1998). In addition, stress was reported to alter neutrophil and macrophage microbicidal functions (Ehrchen et al., 2007; Khanfer et al., 2010; Palermo-Neto et al., 2003). Previous studies in a murine model of cutaneous healing showed that restraint stress increased susceptibility to opportunistic infection. Rojas et al. (2002), reported that even though

bacterial levels were similar at the time of wounding and 6 h post-wounding, under stress, bacterial clearance was impaired leading to increased bacterial load as early as day 1 after wounding, and up to a 3-log increase in bacterial counts at day 5 post-wounding.

We hypothesized that restraint stress alters recruitment and/or functions of neutrophils and macrophages during wound healing, thereby impairing bacterial clearance. The effect of restraint stress on neutrophil and macrophage recruitment and chemokine gene expression during wound healing was investigated. Anti-microbial functions of neutrophils and macrophages were assessed. The expression of cell surface markers that are involved in adhesion and bacterial recognition by macrophages was also examined. Finally, we explored how restraint stress altered the subpopulations of activated macrophages during wound healing.

2. Methods

2.1. Animals

For all animal experiments in this study, we selected the SKH-1e mouse strain, which are hairless. This mouse has been used widely in wound healing models, dermal research/ photosensitivity studies, and safety and efficacy testing. Hairless mice are more susceptible to wounds from fighting because of their relative lack of fur. Female mice are less aggressive and are less likely to develop non-experimental wounds inflicted by littermates during establishment of the litter social hierarchy. Therefore we selected female SKH-1e mouse for the study. In this study, eight-week old female SKH-1e mice were obtained from Charles Rivers, Inc. (Wilmington, MA). Mice were housed in conventional cages, five animals per cage, under a 12:12 light:dark cycle (starting at 18:00), before and throughout the experiments. Water and food were available ad libitum. Animals were allowed 1–2 weeks to acclimate to the cages 7–10 days before the start of the experiment. Animals were handled according to a protocol approved by the Institutional Animal Care and Use Committee.

2.2. Restraint stress

Restraint stress paradigm was used to induce stress in randomly assigned mouse groups. This model provides a consistent physiological and psychological stress response (Sheridan et al., 1991; Zhang et al., 1998; Padgett et al., 1998; Rojas et al., 2002). Each mouse subjected to restraint was placed in a well-ventilated 50 mL conical tube for 12 h/cycle during the active phase. Mice were restrained for three cycles prior to wounding, and five additional cycles after wounding as previously described by Williams et al. (2012), Gajendrareddy et al. (2005). The restraint tubes were cleaned and sterilized between each restraint cycles. Since animals in the tubes did not have access to food and water, control mice were deprived of food and water during the same 12 h periods but were allowed to roam free. As it is well established that restraint stress induces a delay in wound closure (Padgett et al., 1998; Horan et al., 2005; Eijkelkamp et al., 2007), each wound was photographed everyday for each animal, beginning on the day of wounding and analyzed by photoplanimetry. The wound size was determined in order confirm the delay in wound closure in the stressed group, for each experiment (data not shown).

2.3. Wounding and tissue harvest

Mice were anesthetized with 250 μL doses of ketamine-xylazine-saline soluttion (ratio 4:1:35) consisting of ketamine 100 mg/kg and xylazine 5 mg/kg, administrated intra-peritoneally. The dorsal skin was cleaned with isopropanol pads and two full-thickness wounds were created below the shoulder blades using a sterile 3.5 mm biopsy punch (Miltex Inc., York, PA). Mice were anesthetized and the wounds were harvested one and five days

post-wounding with a 6 mm biopsy punch (Miltex Inc., York, PA) before the mice were euthanized.

2.4. Measurement of bacteria load in the wound

Bacterial load at the wound was assessed by methods adapted from Rojas et al. (2002). To harvest wounds for bacterial assays, mice were anesthetized (as described above) and wounds were harvested 5 days post-wounding via 6 mm punch biopsy, and homogenized in 1 mL of sterie 1×PBS, using a Tissue-Tearor (Cole-Parmer, Vernon Hills, IL). Serial dilutions (1:10) were plated, in duplicate, on brain–heart-infusion agar (Becton–Dickinson), incubated for 24 h at 37 °C, and quantified by counting the number of colonies formed.

2.5. Myeloperoxidase (MPO) assay

As described by Zhou et al. (1996), harvested wounds were homogenized in 1 mL of 50 mM sodium phosphate buffer, pH 6.0, with 0.5% HTAB (Sigma–Aldrich, St. Louis, MO). Homogenates were centrifuged at 12,000g for 20 min and underwent 3 cycles of freeze/thaw for MPO extraction. Supernatants were mixed 1:15 with 80 mM sodium phosphate buffer pH 5.4, containing 16 mM 3,5,3′,5′-tetramethylbenzidine (TMB) (Sigma) previously dissolved in dimethylformamide (Sigma–Aldrich, St. Louis, MO). Reactions were started by adding 0.03% hydrogen peroxide, incubated for 2 min at 37 °C, and stopped by adding 200 mM sodium phosphate buffer pH 3.0. Absorbance was measured at 650 nm for each sample. Units of MPO per wound were determined by regression analysis using a standard curve determined with commercial MPO (Sigma–Aldrich, St. Louis, MO), with concentrations of 0.5– 0.0025 units/mL (Schierwagen et al., 1990).

2.6. Macrophage quantification

Formalin-fixed wounds were sectioned at 5 μm and incubated overnight at 4 °C with rat anti-mouse Mac-3 antibody at dilution 1:800 (Pharmingen, San Diego, CA) (Ho and Springer, 1983). Anti-rat Vectostain ABC kit was used following the manufacturer's protocol to allow for detection. The tissues were counterstained with hematoxylin. A blinded observer counted the number of Mac-3 positive and total cells in three different fields (magnification ×40) for each section. The average percentage of Mac-3 + cells was determined and expressed as mean ± SEM as previously described (Engelhardt et al., 1998).

2.7. Total RNA isolation

Harvested tissues were stored in RNAlater® (Sigma–Aldrich, St. Louis, MO) at 4 °C and later homogenized in TRIzol® (Invitrogen, Grand Island, NY) using a Tissue-Tearor (Cole-Parmer, Vernon Hills, IL). Total RNA extraction was completed by chloroform extraction, RNA precipitation in isopropanol, RNA washing with 75% ethanol and dissolving in 20 μL of DPEC-treated water. Spectrophotometry of RNA samples was done at absorbance wavelengths of 260 and 280 nm. A260/280 ratios were used to calculate the total RNA concentration and purity.

2.8. Reverse transcription

Synthesis of cDNA was performed using SuperScript™ First Strand Synthesis System for RT–PCR (Invitrogen, Grand Island, NY). One microgram total RNA was added to 2 μL of random hexamers (50 ng/μL) and 1 μL of 10 mM dNTPs and incubated at 65 °C for 5 min in a GeneAmp® PCR System 2700 (Applied Biosystems). A mixture of 2 μL of 10 × RT buffer, 4 μL of 25 mM $MgCl_2$, 2 μL of 0.1 M DTT and 1 μL of recombinant ribonuclease inhibitor was added to each reaction tube, briefly vortexed, centrifuged, and incubated at 25 °C for 2 min. Then, 1 μL of SuperScript™ II RT (reverse transcriptase) was added to the tubes and thermocycled at 25 °C for 10 min, 42 °C for 50 min, and 70 °C for 15 min. cDNA

synthesis was completed after digestion with 1 μL of RNase H for 37 °C for 20 min to remove residual RNA from the cDNA:RNA hybrid.

2.9. Real-time reverse transcription PCR analysis

Amplification of target cDNA was accomplished using the ABI Prism 7000 Sequence Detection System. Real-time PCR primers and probes were purchased from Applied Biosystems TaqMan® Gene Expression Assays for mouse MIP-1a (#4331182-Mm00441259_g1) MIP-2 (#4331182-Mm00436450_m1), MCP-1 (#4331182-Mm00441242_m1), KC (#4331182-Mm04207460_ m1), CXCL10 (#4331182-Mm00445235_m1), CCL5 (#4331182-Mm01302427_m1), CCL22 (#4331182-Mm00436439_m1), RELMα (#4331182-Mm00445109_m1), IGF-1 (#4331182-Mm00439560_ m1), CCL1 (#4331182-Mm00441236_m1), IL10 (#4331182-Mm00439614_m1) and CD68 (#4331182-Mm03047340_m1) and GAPDH ((#4331182-Mm99999915_g1). Two microliters of cDNA diluted 1:10 were added to 12.5 μL of PE Master Mix (PE Biosystems), 2.5 μL target gene probe-primer mix, 5.5 μL of DEPC-treated water, and 2.5 μL of GAPDH probe and primer mix. The relative amount of target cDNA in each sample was determined by measuring fluorescence of the probe specific for each gene and determining the ΔRn/Ct. Gene expression data were calculated and presented as the relative difference in mRNA levels compared to control. The value is expressed as a ratio of mRNA of gene of interest/mRNA of housekeeping gene (GAPDH).

2.10. Preparation of tissue extract

Wounds harvested one and 5 days post-wounding from control and stressed animals were homogenized on ice using a Tissue-Tearor (Cole-Parmer, Vernon Hills, IL). 1xPBS, 0.5% Tween-20 and mM EDTA supplemented with Protease inhibitor cocktail (Sigma–Aldrich, St. Louis, MO, Cat# P-2714). Tissue homogenates were sonicated and centrifuged at 10000 rpm for 5 min. The supernatants were collected, aliquoted. The protein concentrations were determined by Bio-Rad Protein Assay (Bio-Rad, Hercules, CA).

2.11. Detection of protein levels

The protein concentrations of MIP-2 and CCL5 in the wounds of control and stressed animals were determined using MILLIPLEX MAP Mouse Cytokine/Chemokine Magnetic Bead Panel (Millipore, Billerica, MA) according to the manufacturer's instructions. The OD of IGF-1 per μg of total protein from tissue extract was measured using mouse IGF-1 ELISA from Signosis, Inc. (Sunnyvale, CA) according to the manufacturer's instructions.

2.12. Phagocytic activity and superoxide production

Blood was collected by cardiac puncture and aliquoted 0.5 mL in 5 mL tubes containing final concentration of 10 units/mL of heparin (Elkins-Sinn, Inc., Cherry Hill, NJ). Phagotest® was used according to the manufacturer's protocol to quantify the phagocytic activity of monocytes and granulocytes. This protocol was modified to load neutrophils and macrophages with the reagent to measure oxidative burst by adding dihydroethidium (DHE) (Biotium, Inc., Hayward, CA) at 2.5 μg/mL and incubating for 30 min at 37 °C on a shaker. Live YFP- *Escherichia coli* (kind gift from Dr. Ye from the College of Medicine, UIC) was added to test the phagocytic activity. Fluorescence was quenched by adding Trypan blue pH 7.0 at 4 mg/mL for one minute to each tube before analysis with Beckman Coulter Cyan II.

2.13. Cell surface marker analysis

Blood was collected in the presence of heparin as previously described. One volume of blood was mixed with 20 volumes of pre-warmed 1 × BD™ Phosflow Lyse/Fix buffer (BD Biosciences) and incubated at 37 °C in a water-bath for 10 min. Samples were centrifuged at

500g for 8 min, the supernatant was aspirated and the pellet washed with 1× PBS. The tubes were vortexed to loosen the pellets and the appropriate amounts of conjugated antibodies were added to the tubes (F4/80-APC, CD284-PE, CD11b-FITC (eBioscience, San Diego, CA), CD206-Alexa Fluor® 488 (BioLegend, San Diego, CA); CD68- Alexa Fluor® 700 (AbD Serotec, Raleigh, NC) following the manufacturer's protocol and incubated on ice for 30 min. The samples were washed with 1 mL 1 × PBS, and centrifuged for 2 min at 2000 rpm. Each pellet was resuspended in 0.5 mL of 4% paraformaldehyde and analyzed using Beckman Coulter CyAn II. Cells were gated using SS versus Pulse Width to exclude aggregates, then gated using SS versus FS to exclude debris and select for appropriate cell size. Gating selected F4/80 + cells, which were further gated to select cells double-positive for F4/80 and either CD11b or CD284 or CD68 or CD206.

2.14. Immunohistochemistry and laser capture microdissection

Harvested wounds were embedded in HistoPrep™ (Thermo Fisher Scientific Inc., Waltham, MA) and stored at −80 °C. Frozen sections were cut at 6 μm thickness and mounted on Membrane-Slides PEN-Membrane 2.0 μm (MicroDissect GmbH). The Trogan et al. (2002) staining protocol was followed for immunochemistry staining of macrophages using rabbit anti-mouse CD68 antibody (Abbiotec, San Diego, CA) and against rabbit Vectastain Elite ABC kit (Vector Laboratories, Inc., Burlingame, CA). The macrophages were microdissection using a Leica LMD7000 Laser Microdissection System. Cells harvested by laser dissection were processed for qRT–PCR using RNAqueous®-MicroKit (Invitrogen, Grand Island, NY).

2.15. Statistical analysis

Statistics were performed using SPSS. Differences between groups over time were assessed using repeated-measurement ANOVA Univariate ANOVA analysis was performed to compare between 2 groups at a single time point. Data represented as mean ± SEM from 3 or more experiments. Statistical significance was determined at $p \leq 0.05$ (*), and *p*-values approaching significance ($0.05 < p < 0.1$) were represented as # (ANOVA).

3. Results

To confirm previous study showing that restraint stress impairs bacterial clearance, the number of bacterial colony forming units present in the wounds in stressed and control animals was determined 5 days post-wounding (Fig. 1). As expected the bacterial load in wounds of stressed groups 5 days post-wounding was more than 4 log10 higher than the bacteria present in control animals ($p < 0.000$).

3.1. Neutrophils accumulate in the wound site under restraint stress

To assess the effects of stress on neutrophil recruitment, myeloperoxidase (MPO), a marker of neutrophil infiltration, was quantified by a colorimetric assay in unwounded tissue and in excisional wounds at 6 h, day 1, day 3, day 5 and day 7 post-wounding. Low levels of MPO were detected in unwounded skin (Day 0) from control and stressed mice (Fig. 2A). In control mice, peak MPO levels were found at day 1 (D1) after wounding, with similar levels in stressed mice. At day 3, stressed mice had significantly increased levels of MPO, while MPO in control started to decline ($p \leq 0.05$). At day 5 (D5) post-wounding, MPO levels were elevated **4**-fold ($p \leq 0.05$) in stressed mice as compared to control mice. By day 7, MPO levels had returned to near control levels in both control and stressed mice.

3.2. Gene expression of neutrophil-attracting chemokines increases during stress-impaired wound healing

To determine whether altered kinetics of neutrophil recruitment was due to chemokine expression, MIP-2 and KC mRNA levels were measured by qRT–PCR in unwounded tissue, and wounds excised at day 1 and day 5 post-wounding in both control and stressed groups. In addition, MIP-2 protein concentration was determined in day 5 wounds of control and stressed animals.

MIP-2 mRNA levels increased during the peak of neutrophil recruitment (D1) in controls, and went back to basal level after 5 days (Fig. 2C). Both MIP-2 mRNA level and protein concentration were higher in stressed groups as compared to control groups at D5 (Fig. 2C and D). KC expression level did not significantly vary over time in control groups during wound healing (Fig. 2B). Similar to MIP-2, KC gene expression increased in stressed mice, approaching significance at D5.

3.3. Restraint stress does not affect macrophage recruitment or the expression of macrophage chemokines at the wound site

To assess the effects of restraint stress on macrophage recruitment, wounds excised at day 1 through day 7 post-wounding were prepared for immunostaining with a monoclonal antibody against murine Mac-3 (Figs. 3 and 4). Fig. 3 shows a representative tissue section from wounds from stressed and control groups one and five days post-wounding. Mac-3 positive (Mac-3+) and total cells were counted, and the average percentage of Mac-3 + cells was determined. Both control and stressed mice had similar macrophage wound infiltration (Fig. 4A). The expression profiles of macrophage chemokines MCP-1 and MIP-1α were examined by qRT–PCR (Fig. 4B and C). MCP-1 mRNA level did not significantly vary over time in either control or stressed groups. MIP-1α relative gene expression increased at D1 compared to unwounded tissue and D5 tissues in control; nevertheless, restraint stress did not affect the expression of MCP-1 and MIP-1α.

3.4. Restraint stress decreases phagocytic activity, but does not affect oxidative burst during wound healing

Phagocytosis and oxidative burst are crucial functions of phagocytic cells for killing pathogens. Phagocytosis activity was assessed by measuring the mean fluorescence intensity emitted by ingested YFP-*E. coli* incubated with whole blood harvested one, three and five days post-wounding (Fig. 5). Interestingly, the mean fluorescence intensity was significantly reduced by 18–30% in stressed mice at all time points as compared to control, suggesting that fewer bacteria were phagocytozed during stress-impaired wound healing. Superoxide production by phagocytic cells was the second key bactericidal function tested. Upon stimulation with *E. coli*, the oxidative burst from phagocytic cells was measured as the mean fluorescence intensity from the release of DHE product. The mean fluorescence intensity did not vary between control and stressed groups at one, three and five days post-wounding.

3.5. Cell surface expression of CD11b and TLR4 is down regulated in stressed mice

The cell surface expression of monocyte/macrophage markers, adhesion molecules and TLR4 was measured by flow cytometry at D1 and D5 post-wounding. F4/80 + monocytes were gated. The mean cell fluorescence for cell surface macrophage marker CD68 did not significantly change under restraint stress (Fig. 6A), and nor did CD62L, a marker involved in leukocyte rolling and homing (data not shown). Interestingly, the cell surface expression of CD11b, which regulates migration and participates in cell adhesion to bacteria, was lowered by 43% at D1 in stressed animals ($p = 0.002$) as compared to control. Fig. 6B represents the shift in the curve of the mean cell fluorescence intensity for CD11b between

control and stressed groups observed at D1. TLR4 (CD284), which recognizes Gram (−) bacteria and triggers pro-inflammatory response, was expressed 35% less at D1 in stressed group as compared to control ($p = 0.018$) (Fig. 6A). Cell surface expression of mannose receptor (CD206), which is a marker of alternatively activated macrophages, was not affected by stress.

3.6. Gene expression of CAM and WHM markers and the regulatory macrophage marker CCL1 are reduced in stressed groups, whereas IL-10 gene expression increases

To investigate the effect of stress on the phenotype of activated macrophages present at the wound site, gene expression of markers of CAM (CXCL10, CCL5 and TLR4), WHM (CCL22, RELMα and IGF-1) and regulatory macrophages (CCL1 and IL10) were measured by qRT–PCR in unwounded tissue and wounds from D1 and D5. In addition, the protein concentration of CCL5 relative to total protein concentration at in day1 and day 5 wounds was determined in control and stressed groups.

Both CXCL10 and CCL5 mRNA levels were down regulated in unwounded tissue and D1 wounds for CCL5, and D1 only for CXCL10 (Fig. 7A and B). Similarly CCL5 protein concentration was significantly lower in wounds of stressed animals at day 1 compared to controls ($p = 0.004$) (Fig. 7C). TLR4 gene expression was not differentially regulated under stress (data not shown).

mRNA levels of CCL22 and IGF-1, which are markers of WHM, were significantly lower in stressed mice at D1 and D5 post-wounding with a 6-fold decrease in CCL22, and a 3-fold decrease in IGF-1 at both D1 and D5 respectively (Fig. 8). IGF-1 relative protein concentration was similarly lower in the wounds of stressed animals at days 1 and 5 (Fig. 8D).

Interestingly, mRNA levels of RELMα decreased 6-fold in unwounded tissue in stressed groups as compared to the controls ($p \leq 0.05$). The cytokines IL-4 and IL-13, reported to induce WHM, were not detected by qRT–PCR in the whole wound (data not shown). The mRNA levels of Arginase-1 did not significantly vary in the wounds of stressed animals compared to control group (data not shown).

The regulatory macrophage marker CCL1 was increased at the mRNA level at D5 post-wounding in the controls; whereas under restraint stress, its gene expression was 8-fold and 12-fold lower at D1 and D5, respectively (Fig. 9). IL-10 gene expression increased over time in stressed mice, and at D5 the mRNA level of this anti-inflammatory cytokine was significantly higher in stressed than control mice ($p \leq 0.05$).

To further confirm the previous data from whole wounds, macrophages were harvested from wound sections of control and stressed mice at D5 using laser capture microdissection, which allows single cell dissection. Gene expression of IGF-1 was measured and expressed as a ratio against the macrophage marker CD68 (Fig. 10). As expected, IGF-1 gene expression from dissected macrophages reflected previous results from the whole wound; the ratio of IGF-1 mRNA to CD68 mRNA was higher in macrophages from control as compared to stressed animals.

4. Discussion

Restraint stress has been shown to increase susceptibility to opportunistic infection. This study investigated the effect of stress on neutrophils and macrophages, which are responsible for bacterial clearance. The results show that impaired bacterial clearance observed as early as day one post-wounding under restraint stress (Rojas et al., 2002) cannot

be attributed to a reduced neutrophil recruitment. Restraint stress did not alter the number of neutrophils during the early stage of healing (day 1 post-wounding) when the highest number of neutrophils is found in the control group. However, stress led to increased neutrophil accumulation at days 3 and five of the healing process. It is well established that neutrophil infiltration mirrors bacterial number, therefore, the increased bacterial load under stress may be driving neutrophil recruitment. The pattern of neutrophil presence in the wound parallels the pattern of bacterial numbers and similar to bacterial numbers, neutrophils are reduced to control levels by day 7, after stress removal. MIP-2 and KC gene expression were increased at day 5, which is consistent with prolonged neutrophil infiltration. Similarly Sakamoto et al. (1996) found increased mRNA expression of the rat homologue of KC in the brain after immobilization stress. These results are in contrast to the Rovai et al. (1998), which observed insensitivity of MIP-2 and KC to regulation by the stress hormone glucocorticoid. Liu et al. (1999) previously demonstrated that glucocorticoids prolonged neutrophil viability for 12–48 h *in vitro*. The excessive infiltration and/or longer retention of neutrophils at the wound might further tissue damage by the release of oxidants and hydrolytic enzymes from activated neutrophils. In addition, Zheng et al. (2004), reported that ingestion of apoptotic neutrophils actively suppresses stimulation of macrophages, which may alter macrophage response. The mechanism(s) resulting in neutrophil accumulation (increased recruitment and/or longer life-span) should be investigated. Our data on neutrophil presence in the wound further emphasized the crucial role of macrophages in bacterial clearance.

Macrophage recruitment and gene expression of chemokines MIP-1α and MCP-1 were not significantly affected by restraint stress during wound healing. The strong presence of neutrophils at a later time during which macrophage population in the tissue is unchanged might overwhelm the macrophages in charge of removing apoptotic neutrophils. This effect might lead to additional tissue damage and would impair the resolution of inflammation. Interestingly, studies on the effects of stress on phagocytic cell accumulation have yielded conflicting results. Bilbo et al. (2002) reported that after 2 h of restraint, increased numbers of neutrophils and monocytes accumulated in a surgical sponge implanted in a mouse, whereas Zhang's team reported that restraint suppressed the migration of neutrophils and macrophages into the peritoneal cavities after IP inoculation of Listeria monocytogenes (1998). These differences between studies may come from the type of stress, namely acute stress (Bilbo et al., 2002) versus chronic stress, as well as the presence of a large number of bacteria in Zhang's model of *L. monocytogenes* infection. The present study measured the recruitment of macrophages in a naturalistic model wound healing in a model that represents a more persistent stressor.

Even though stress did not affect macrophage presence in the wounded tissue, how stress may differentially regulate macrophage phenotype and function in the blood and the wound during healing was investigated. Our results showed that stress diminished the phagocytic ability of the inflammatory cell population in the blood during wound healing; yet restraint stress did not alter the cells' capacity for oxidative burst. Impairment of phagocytic function by stress was similarly observed in the Palermo-Neto et al. (2003) during which mice were exposed to the response delivered by other mice receiving inescapable footshock. Kang et al. (1997) found that examination stress increases superoxide production (1997). Acute psychological stress was reported to increase phagocytic ability and reduce superoxide production of neutrophils in humans (Khanfer et al., 2010), suggesting that the type of stress experienced has different effects on phagocytic abilities. Our current study did not distinguish between the contribution from neutrophil and monocyte/macrophage phagocytosis, which will be investigated later. Harvesting phagocytic cells directly from wounds could provide information about phagocytic and oxidative burst abilities but the isolation process may activate the cells. Oxygen, required for oxidative burst, is less

available at the site of injury due to the disruption of the vascular system and to the stress-induced activation of the sympathetic nervous system and vasoconstriction. Decreasing oxygen delivery could potentially impair bacteria clearance, yet preliminary studies do not indicate that supplementing oxygen systemically decreases bacterial load.

In the blood, CD11b cell surface expression of circulating monocytes/macrophages was down-regulated at day 1 post-wounding under stress, whereas CD68 and CD62L levels did not vary. CD11b is involved in leukocytes' rolling, homing and bacteria recognition. Even though low CD11b expression may have slowed down cell trafficking, macrophage recruitment was not altered. Stress also decreased TLR4 (CD284) cell surface expression during inflammation. Similarly, Du et al. (2010) reported that stress hormones such as corticosterone and epinephrine induced down-regulation of TLR4 in macrophages *in vitro*. CD11b and TLR4 decreased expression could potentially impede bacteria recognition and binding by macrophages.

TLR4 binding to LPS triggers activation of classically activated macrophages, which are highly efficient in bacterial killing and in promoting a pro-inflammatory response. In tissue, TLR4 gene expression was unchanged, however, the mRNA levels of other markers of classically activated macrophages, such as CXCL10 and CCL5, were decreased in the stressed group. Our data is in agreement with the study of Ehrchen et al. (2007) that showed that treatment of human monocytes with glucocorticoids for 2 h led to the down-regulation of CXCL10 and CCL5 *in vitro*.

Expression of the markers for wound-associated macrophages CCL22 and IGF-1 declined under stress at day 1 and day 5 post-wounding. Dissection of macrophages from wounds of control and stressed mice at day 5 confirmed IGF-1 down-regulation. IGF-1 induces keratinocyte and fibroblast proliferation and migration (Lee et al., 2010). Over-expression of IGF-1 in mouse keratinocytes increased their proliferation and migration, which improved wound healing (Semenova et al., 2008). This suggests that an IGF-1-decreased expression under stress would have detrimental effects on wound closure and tissue repair. In addition, lower RELMα expression was observed in the stressed group before wounding occurred, suggesting that restraint stress also alters the deposition of extracellular matrix. It is worth pointing out that even though IL4/IL13 were reported to be necessary for the development of the wound-healing macrophage phenotype (Mosser and Edwards, 2008), IL4 and IL13 could not be detected in the wound in either the control or the stressed groups in this study. This observation supports similar findings by Daley et al. (2010) and Bryan et al. (2005) groups.

Stress also dysregulated gene expression of markers of regulatory macrophages, which promote the resolution of inflammation. The mRNA level of CCL1 decreased at D1 and D5 in the whole wounds of the stressed group, whereas gene expression of IL10 increased as previously shown by Curtin and Sesti-Costa's groups (Curtin et al., 2009; Sesti-Costa et al., 2012).

During normal tissue repair, the macrophage phenotype evolves from a pro-inflammatory phenotype of CAM to a less-inflammatory/anti-inflammatory phenotype that is characteristic of WHM and regulatory macrophages. In diabetic db/db mice, the pro-inflammatory phenotype persisted through 10 days post-injury (Mirza and Koh, 2011). This group reported that dysregulation of macrophage phenotypes contributes to impaired healing in a diabetic mouse model. Interestingly, our study shows that stress did not promote a shift of the macrophage population, but did dysregulate the gene expression of markers of all three of the macrophage populations present during wound healing without a significant decrease in macrophage numbers. The mechanism behind this general dampening of

macrophage phenotype and function is unclear. Macrophage dysregulation by stress, in addition to the dampening of macrophage function resulting from excessive neutrophil phagocytosis, could contribute to impaired bacterial clearance.

Studying the expression of markers linked to macrophage activation in the whole wound enabled the determination of how stress affects the macrophage environment, and influences the phenotype. The LCM study focused on gene expression of isolated macrophages. Our work highlights the need to explore multiple markers of macrophage activation in order to understand the complexity of macrophage phenotypes involved in wound healing.

Altogether, our findings suggest that stress-induced impaired bacterial clearance is in part due to altered phagocytic abilities of neutrophils and macrophages. In addition, stress impacts macrophage activation by inducing the overall dysregulation of macrophage response during tissue repair. A better understanding of the mechanisms behind normal transition of macrophage phenotype during wound healing would provide crucial information to resolve stress-induced changes in macrophage phenotype with the goal to dysregulate their activation in order to ameliorate bacterial clearance and wound healing. Modulation of the macrophage phenotype could provide a new therapeutic approach in the clinical treatment of impaired wound healing.

Acknowledgments

We thank Dr. Leah Pyter for her help with FACS analysis, Dr. Ye for providing YFP-*E. coli*, Dr. Koh for his helpful advice. This project was supported by NIH/NIDCR Grant DE-017686.

References

Bilbo SD, Dhabhar FS, Viswanathan K, Saul A, Yellon SM, Nelson RJ. Short day lengths augment stress-induced leukocyte trafficking and stress-induced enhancement of skin immune function. Proc. Natl. Acad. Sci. USA. 2002; 99:4067–4072. [PubMed: 11904451]

Bryan D, Walker KB, Ferguson M, Thorpe R. Cytokine gene expression in a murine wound healing model. Cytokine. 2005; 31:429–438. [PubMed: 16102971]

Bullard DC, Kunkel EJ, Kubo H, Hicks MJ, Lorenzo I, Doyle NA, Doerschuk CM, Ley K, Beaudet AL. Infectious susceptibility and severe deficiency of leukocyte rolling and recruitment in E-selectin and P-selectin double mutant mice. J. Exp. Med. 1996; 183:2329–2336. [PubMed: 8642341]

Curry JM, Hanke ML, Piper MG, Bailey MT, Bringardner BD, Sheridan JF, Marsh CB. Social disruption induces lung inflammation. Brain Behav. Immun. 2010; 24:394–402. [PubMed: 19903521]

Curtin NM, Mills KH, Connor TJ. Psychological stress increases expression of IL-10 and its homolog IL-19 via beta-adrenoceptor activation: reversal by the anxiolytic chlordiazepoxide. Brain Behav. Immun. 2009; 23:371–379. [PubMed: 19159673]

Daley JM, Brancato SK, Thomay AA, Reichner JS, Albina JE. The phenotype of murine wound macrophages. J. Leukoc. Biol. 2010; 87:59–67. [PubMed: 20052800]

DiPietro LA, Burdick M, Low QE, Kunkel SL, Strieter RM. MIP-1alpha as a critical macrophage chemoattractant in murine wound repair. J. Clin. Invest. 1998; 101:1693–1698. [PubMed: 9541500]

Du Q, Min S, Chen LY, Ma YD, Guo XL, Wang Z, Wang ZG. Major stress hormones suppress the response of macrophages through down-regulation of TLR2 and TLR4. J. Surgical Res. 2010; 173(2):354–361.

Edwards JP, Zhang X, Frauwirth KA, Mosser DM. Biochemical and functional characterization of three activated macrophage populations. J. Leukoc. Biol. 2006; 80:1298–1307. [PubMed: 16905575]

Ehrchen J, Steinmuller L, Barczyk K, Tenbrock K, Nacken W, Eisenacher M, Nordhues U, Sorg C, Sunderkotter C, Roth J. Glucocorticoids induce differentiation of a specifically activated, anti-inflammatory subtype of human monocytes. Blood. 2007; 109:1265–1274. [PubMed: 17018861]

Eijkelkamp N, Engeland CG, Gajendrareddy PK, Marucha PT. Restraint stress impairs early wound healing in mice via alpha-adrenergic but not beta-adrenergic receptors. Brain Behav. Immun. 2007; 21:409–412. [PubMed: 17344022]

Engelhardt E, Toksoy A, Goebeler M, Debus S, Brocker EB, Gillitzer R. Chemokines IL-8, GROalpha, MCP-1, IP-10, and Mig are sequentially and differentially expressed during phase-specific infiltration of leukocyte subsets in human wound healing. Am. J. Pathol. 1998; 153:1849–1860. [PubMed: 9846975]

Filep JG, Delalandre A, Payette Y, Foldes-Filep E. Glucocorticoid receptor regulates expression of L-selectin and CD11/CD18 on human neutrophils. Circulation. 1997; 96:295–301. [PubMed: 9236448]

Gajendrareddy PK, Sen CK, Horan MP, Marucha PT. Hyperbaric oxygen therapy ameliorates stress-impaired dermal wound healing. Brain Behav. Immun. 2005; 19:217–222. [PubMed: 15797310]

Heasman SJ, Giles KM, Ward C, Rossi AG, Haslett C, Dransfield I. Glucocorticoid-mediated regulation of granulocyte apoptosis and macrophage phagocytosis of apoptotic cells: implications for the resolution of inflammation. J. Endocrinol. 2003; 178:29–36. [PubMed: 12844333]

Ho MK, Springer TA. Tissue distribution, structural characterization, and biosynthesis of Mac-3, a macrophage surface glycoprotein exhibiting molecular weight heterogeneity. J. Biol. Chem. 1983; 258:636–642. [PubMed: 6336756]

Horan MP, Quan N, Subramanian SV, Strauch AR, Gajendrareddy PK, Marucha PT. Impaired wound contraction and delayed myofibroblast differentiation in restraint-stressed mice. Brain Behav. Immun. 2005; 19:207–216. [PubMed: 15797309]

Kang DH, Coe CL, McCarthy DO, Jarjour NN, Kelly EA, Rodriguez RR, Busse WW. Cytokine profiles of stimulated blood lymphocytes in asthmatic and healthy adolescents across the school year. J. Interferon Cytokine Res. 1997; 17:481–487. [PubMed: 9282829]

Kernacki KA, Barrett RP, Hobden JA, Hazlett LD. Macrophage inflammatory protein-2 is a mediator of polymorphonuclear neutrophil influx in ocular bacterial infection. J. Immunol. 2000; 164:1037–1045. [PubMed: 10623854]

Khanfer R, Phillips AC, Carroll D, Lord JM. Altered human neutrophil function in response to acute psychological stress. Psychosom. Med. 2010; 72:636–640. [PubMed: 20562369]

Liu Y, Cousin JM, Hughes J, Van Damme J, Seckl JR, Haslett C, Dransfield I, Savill J, Rossi AG. Glucocorticoids promote nonphlogistic phagocytosis of apoptotic leukocytes. J. Immunol. 1999; 162:3639–3646. [PubMed: 10092825]

Martinez FO, Sica A, Mantovani A, Locati M. Macrophage activation and polarization. Front Biosci. 2008; 13:453–461. [PubMed: 17981560]

Maus U, Herold S, Muth H, Maus R, Ermert L, Ermert M, Weissmann N, Rosseau S, Seeger W, Grimminger F, Lohmeyer J. Monocytes recruited into the alveolar air space of mice show a monocytic phenotype but upregulate CD14. Am. J. Physiol. Lung Cell. Mol. Physiol. 2001; 280:L58–L68. [PubMed: 11133495]

Mercado AM, Quan N, Padgett DA, Sheridan JF, Marucha PT. Restraint stress alters the expression of interleukin-1 and keratinocyte growth factor at the wound site: an in situ hybridization study. J. Neuroimmunol. 2002; 129:74–83. [PubMed: 12161023]

Mirza R, Koh TJ. Dysregulation of monocyte/macrophage phenotype in wounds of diabetic mice. Cytokine. 2011; 56:256–264. [PubMed: 21803601]

Mizobe K, Kishihara K, Ezz-Din El-Naggar R, Madkour GA, Kubo C, Nomoto K. Restraint stress-induced elevation of endogenous glucocorticoid suppresses migration of granulocytes and macrophages to an inflammatory locus. J. Neuroimmunol. 1997; 73:81–89. [PubMed: 9058763]

Mosser DM, Edwards JP. Exploring the full spectrum of macrophage activation. Nat. Rev. Immunol. 2008; 8:958–969. [PubMed: 19029990]

Padgett DA, Marucha PT, Sheridan JF. Restraint stress slows cutaneous wound healing in mice. Brain Behav. Immun. 1998; 12:64–73. [PubMed: 9570862]

Palermo-Neto J, de Oliveira Massoco C, Robespierre de Souza W. Effects of physical and psychological stressors on behavior, macrophage activity, and Ehrlich tumor growth. Brain Behav. Immun. 2003; 17:43–54. [PubMed: 12615049]

Rodero MP, Khosrotehrani K. Skin wound healing modulation by macrophages. Int. J. Clin. Exp. Pathol. 2010; 3:643–653. [PubMed: 20830235]

Rojas IG, Padgett DA, Sheridan JF, Marucha PT. Stress-induced susceptibility to bacterial infection during cutaneous wound healing. Brain Behav. Immun. 2002; 16:74–84. [PubMed: 11846442]

Rovai LE, Herschman HR, Smith JB. The murine neutrophil-chemoattractant chemokines LIX, KC, and MIP-2 have distinct induction kinetics, tissue distributions, and tissue-specific sensitivities to glucocorticoid regulation in endotoxemia. J. Leukoc. Biol. 1998; 64:494–502. [PubMed: 9766630]

Sakamoto Y, Koike K, Kiyama H, Konishi K, Watanabe K, Tsurufuji S, Bicknell RJ, Hirota K, Miyake A. A stress-sensitive chemokinergic neuronal pathway in the hypothalamo–pituitary system. Neuroscience. 1996; 75:133–142. [PubMed: 8923529]

Savill J. Apoptosis in resolution of inflammation. J. Leukoc. Biol. 1997; 61:375–380. [PubMed: 9103222]

Schierwagen C, Bylund-Fellenius AC, Lundberg C. Improved method for quantification of tissue PMN accumulation measured by myeloperoxidase activity. J. Pharmacol. Methods. 1990; 23:179–186. [PubMed: 2158602]

Semenova E, Koegel H, Hasse S, Klatte JE, Slonimsky E, Bilbao D, Paus R, Werner S, Rosenthal N. Overexpression of mIGF-1 in keratinocytes improves wound healing and accelerates hair follicle formation and cycling in mice. Am. J. Pathol. 2008; 173:1295–1310. [PubMed: 18832567]

Sesti-Costa R, Ignacchiti MD, Chedraoui-Silva S, Marchi LF, Mantovani B. Chronic cold stress in mice induces a regulatory phenotype in macrophages: correlation with increased 11beta-hydroxysteroid dehydrogenase expression. Brain Behav. Immun. 2012; 26:50–60. [PubMed: 21801831]

Sironi M, Martinez FO, D'Ambrosio D, Gattorno M, Polentarutti N, Locati M, Gregorio A, Iellem A, Cassatella MA, Van Damme J, Sozzani S, Martini A, Sinigaglia F, Vecchi A, Mantovani A. Differential regulation of chemokine production by Fcgamma receptor engagement in human monocytes: association of CCL1 with a distinct form of M2 monocyte activation (M2b, Type 2). J. Leukoc. Biol. 2006; 80:342–349. [PubMed: 16735693]

Trogan E, Choudhury RP, Dansky HM, Rong JX, Breslow JL, Fisher EA. Laser capture microdissection analysis of gene expression in macrophages from atherosclerotic lesions of apolipoprotein E-deficient mice. Proc. Natl. Acad. Sci. USA. 2002; 99:2234–2239. [PubMed: 11842210]

Viswanathan K, Dhabhar FS. Stress-induced enhancement of leukocyte trafficking into sites of surgery or immune activation. Proc. Natl. Acad. Sci. USA. 2005; 102:5808–5813. [PubMed: 15817686]

Wetzler C, Kampfer H, Stallmeyer B, Pfeilschifter J, Frank S. Large and sustained induction of chemokines during impaired wound healing in the genetically diabetic mouse: prolonged persistence of neutrophils and macrophages during the late phase of repair. J. Invest. Dermatol. 2000; 115:245–253. [PubMed: 10951242]

Williams RL, Sroussi HY, Abercrombie JJ, Leung K, Marucha PT. Synthetic decapeptide reduces bacterial load and accelerates healing in the wounds of restraint-stressed mice. Brain Behav. Immun. 2012; 26:588–596. [PubMed: 22329957]

Zhang D, Kishihara K, Wang B, Mizobe K, Kubo C, Nomoto K. Restraint stress-induced immunosuppression by inhibiting leukocyte migration and Th1 cytokine expression during the intraperitoneal infection of *Listeria monocytogenes* . J. Neuroimmunol. 1998; 92:139–151. [PubMed: 9916889]

Zheng L, He M, Long M, Blomgran R, Stendahl O. Pathogen-induced apoptotic neutrophils express heat shock proteins and elicit activation of human macrophages. J. Immunol. 2004; 173:6319–6326. [PubMed: 15528371]

Zhou L, Pope BL, Chourmouzis E, Fung-Leung WP, Lau CY. Tepoxalin blocks neutrophil migration into cutaneous inflammatory sites by inhibiting Mac-1 and E-selectin expression. Eur. J. Immunol. 1996; 26:120–129. [PubMed: 8566054]

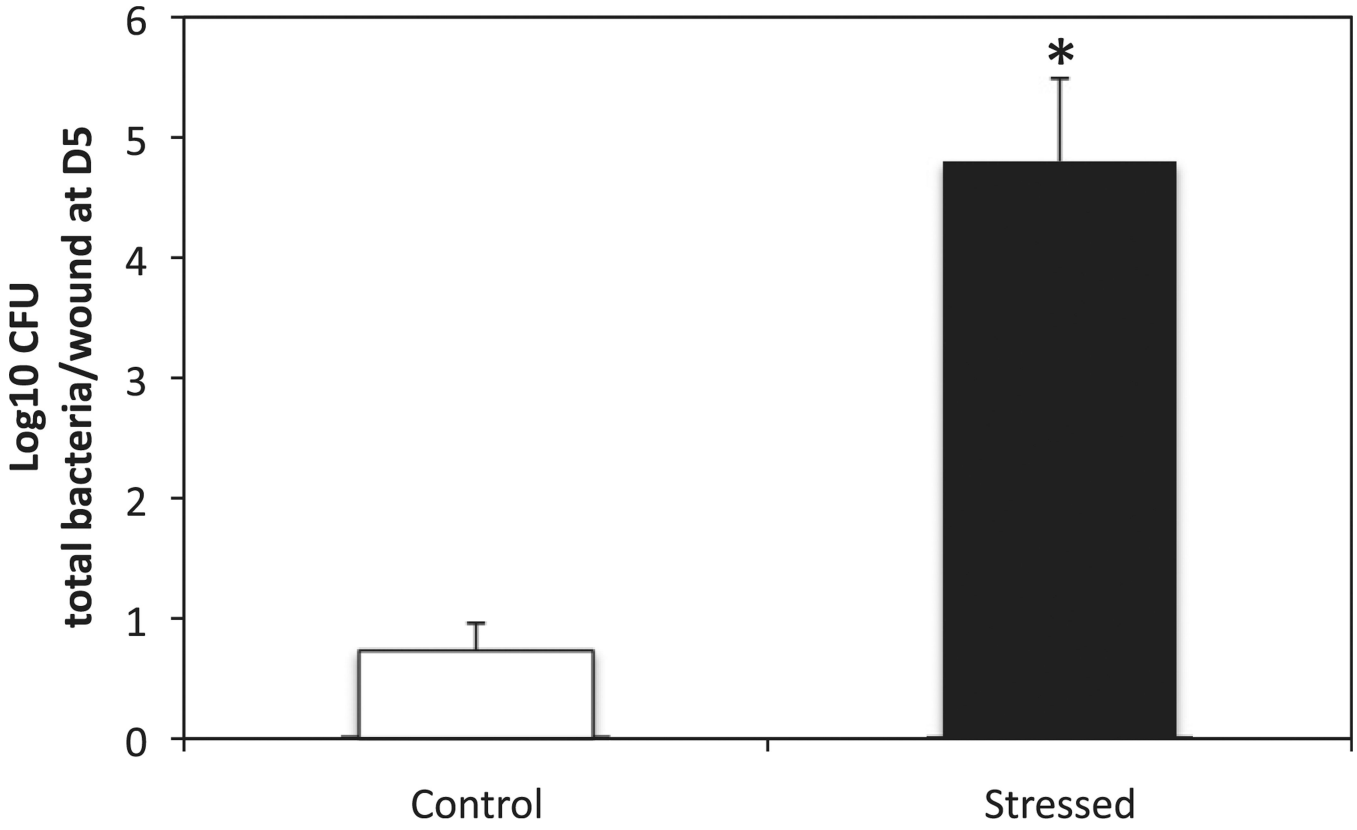

Fig. 1.

Number of bacteria in the wounds of stressed and control animals 5 days post-wounding. Wounds of stressed and control mice were harvested 5 days post-wounding and homogenized in 1 mL PBS. Serial dilutions (1:10) were plated, in duplicate, on brain-heart-infusion agar (Becton-Dickinson), incubated for 24 h at 37 °C. The bacterial load in the wounds was quantified by counting the number of colonies formed. Data represent mean ± SEM from 3 experiments. $n = 15$ mice/group. $^{*}p \leq 0.05$ Stressed mice compared to control (ANOVA).

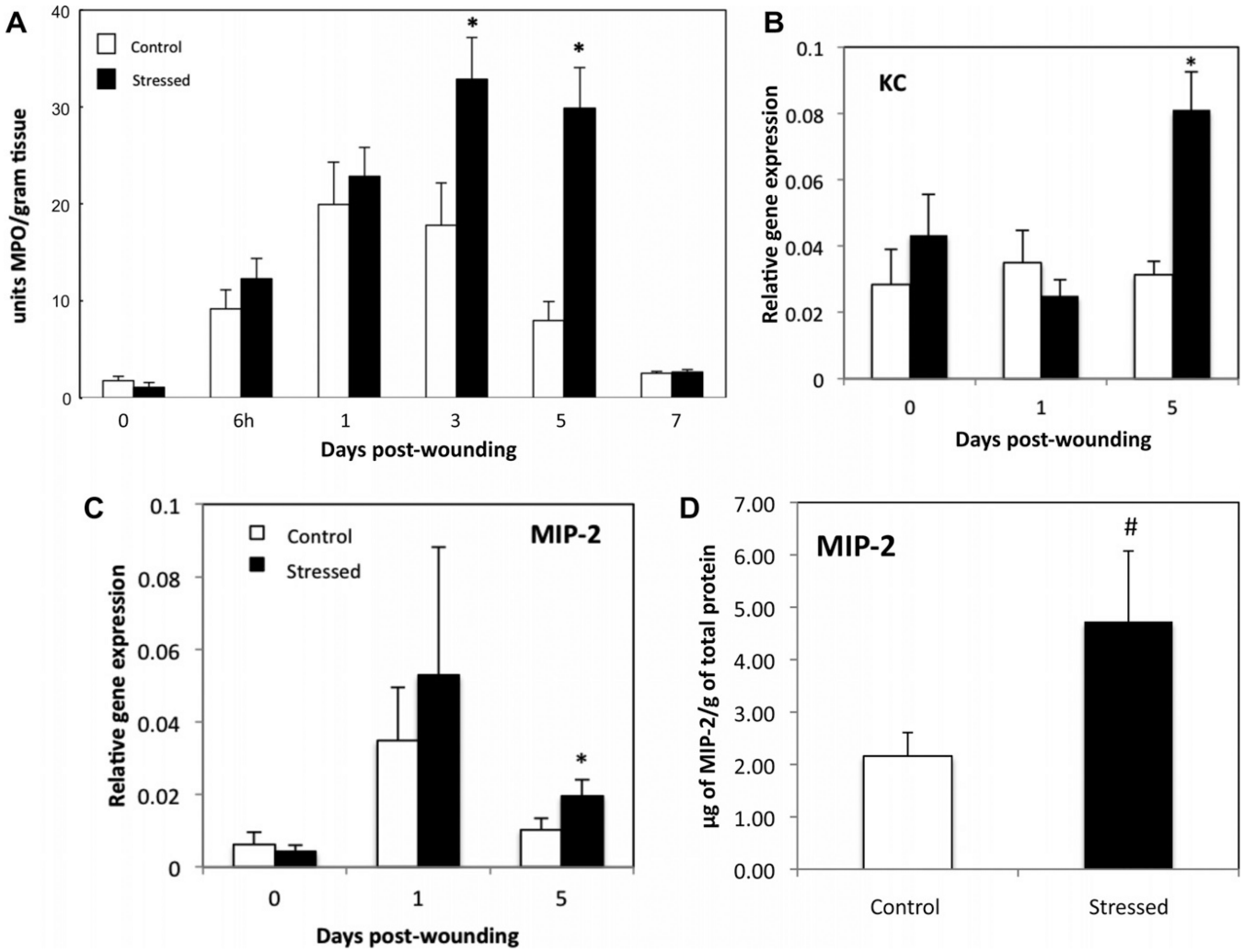

Fig. 2.

Neutrophil recruitment and gene expression of chemokines MIP-2 and KC. Mice were euthanized at 6 h and days 1 through 7 after wounding. Excised wounds and control skin were subjected to myeloperoxidase (MPO) extraction. MPO was quantitated by a colorimetric assay and expressed as units of MPO/gram of wound tissue. Data represent mean ± SEM from 2 pooled experiments. At each time-point, $n = 7–12$ mice/group, except for D7 and control skin ($n = 3–5$). $^{*}p \leq 0.05$ compared to control (ANOVA). (B and C) Unwounded skin and wounds were harvested at 1 and 5 days post-wounding. The gene expressions of KC (B) and MIP-2 (C) were measured and compared to the housekeeping gene GAPDH using qRT–PCR. Data represent mean ± SEM from 4 experiments. At each time point $n = 20$ mice/group. Fig. 2D represents the protein concentration of MIP-2 in µg/g of total protein from tissue extract of day 5 wounds of control and stressed mice. Data represent mean ± SEM from $n = 3–4$ mice/group. $^{*}p \leq 0.05$ and # $0.05 < p < 0.1$ compared to control.

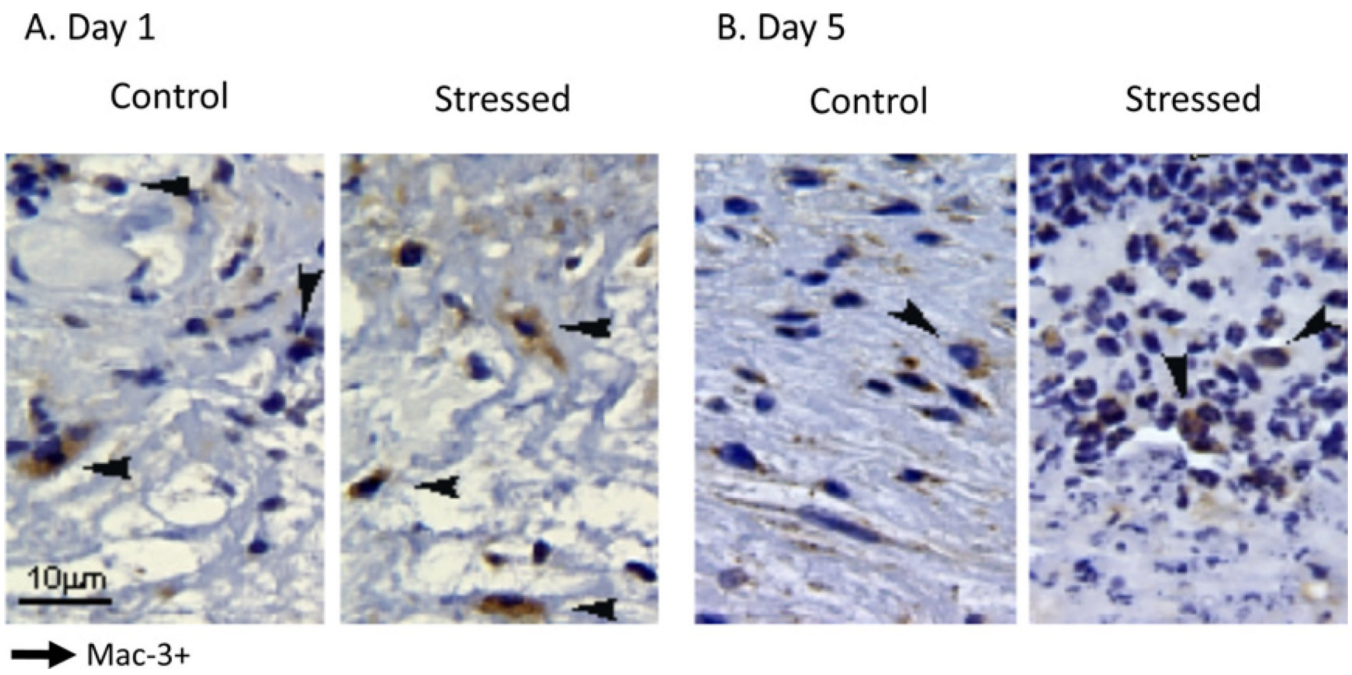

Fig. 3.

Immunohistochemical sections of skin wounds from stressed and control mice at days 1 (A) and 5 (B) after wounding. Wounds were paraformaldehyde-fixed and paraffin-embedded. Wound sections (5 m) were immunostained with a monoclonal antibody specific for activated murine macrophages (Mac-3) and counterstained with hematoxylin. Black arrows indicate Mac-3 positive (Mac-3+) cells. Original magnification ×60.

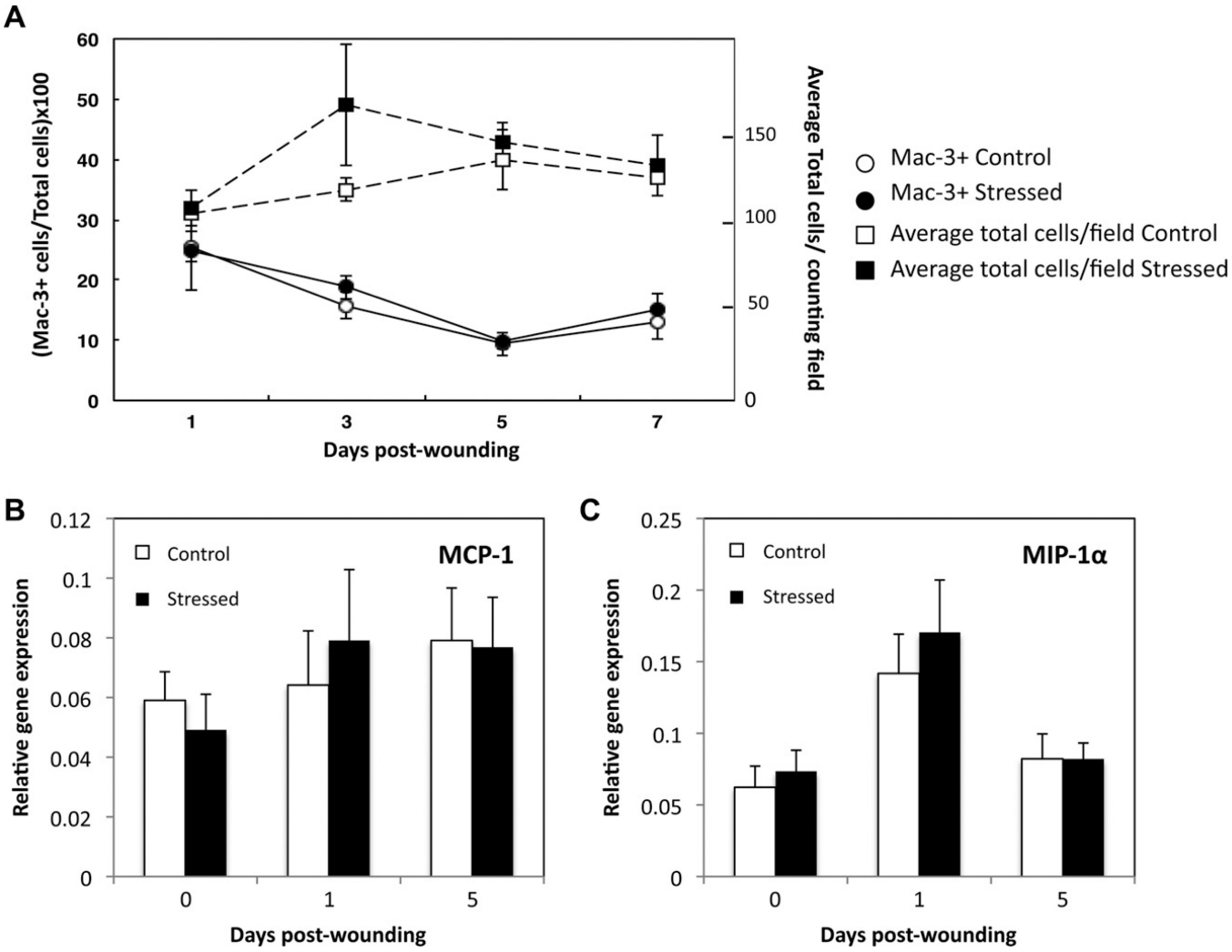

Fig. 4.

Macrophage recruitment and gene expression of chemokines MCP-1 and MIP-1α. Wounds, excised from day 1 through 7 post-wounding, were paraffin-embedded, sectioned and immunostained with a monoclonal antibody against Mac-3. Data represent mean number of cells and mean percentage of Mac-3 + cells per counting field (±SEM) from two pooled experiments. At each time point n = 6–7 mice/group, except for D7 (n = 3). Unwounded skin and wounds were harvested at 1 and 5 days post-wounding. The gene expressions of MCP-1 (B) and MIP-1α (C) were measured and compared to the housekeeping gene GAPDH using qRT–PCR. Data represent mean ± SEM from 4 experiments. At each time point n = 20 mice/group. No significant group differences were found.

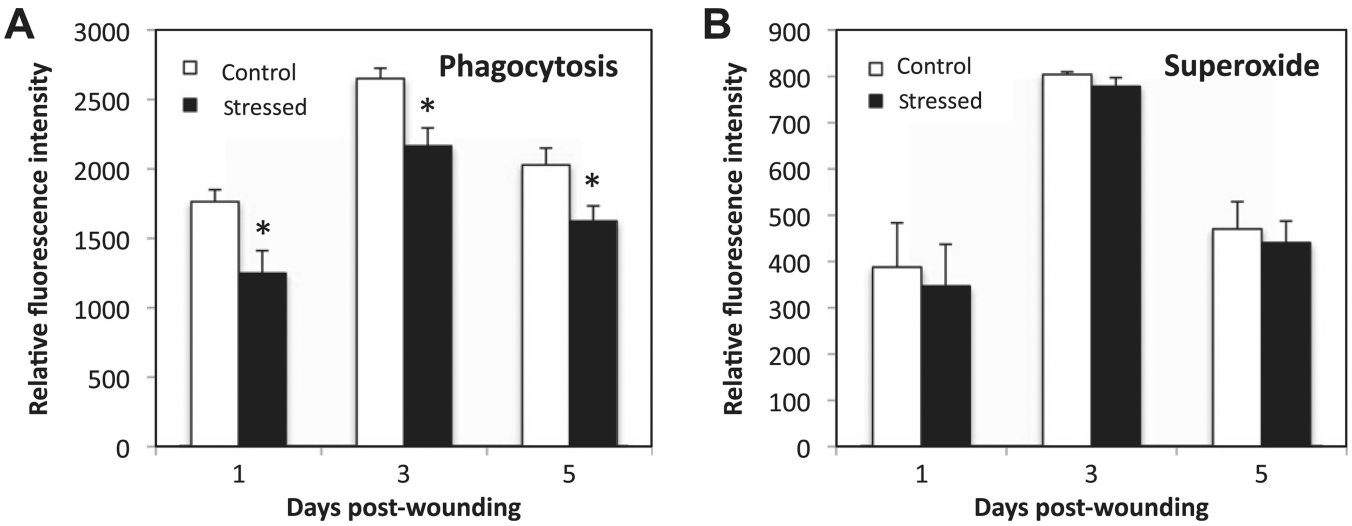

Fig. 5.

Phagocytic activity and superoxide production of phagocytic cells. To measure oxidative burst, DHE (2.5 μ/mL) was added to the heparinized whole blood harvested at D1 and D5. Live YFP-*E. coli* were added to test the phagocytic activity. Mean fluorescence intensity for YFP and DHE were measured. Data represent mean ± SEM from 2–3 experiments. At each time point n = 10–15 mice/group. $^{*}p \leq 0.05$ Compared to control (ANOVA).

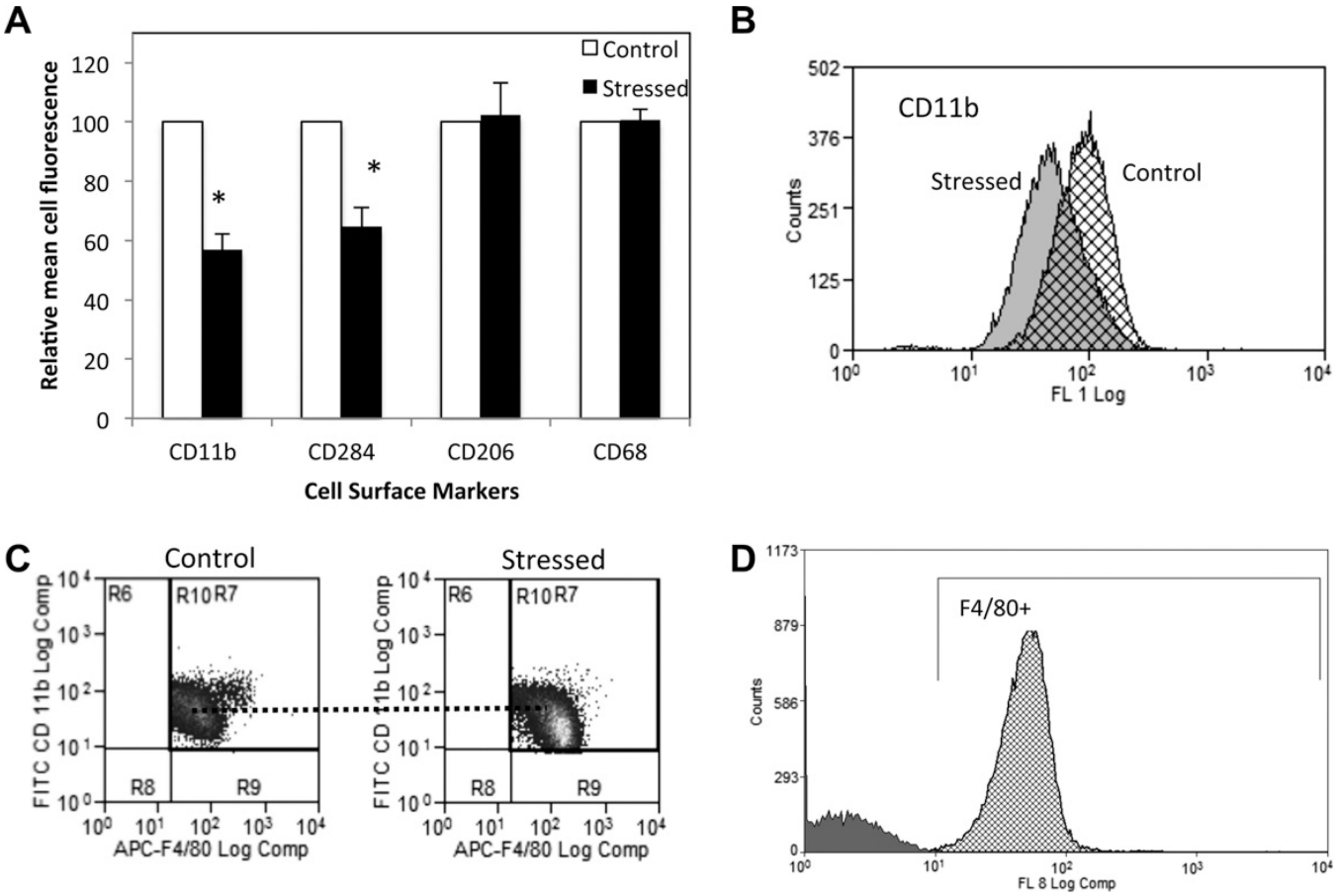

Fig. 6.

Cell surface expression of F4/80 + cells one day post-wounding. F4/80 + cells were gated and the mean cell surface expression for CD11b, CD284, CD206 and CD68 was measured using Beckman Coulter CyAn II. Data represent mean ± SEM from 4 experiments of pooled blood from $n = 5$ mice per condition per experiment $^{*}p \leq 0.05$ compared to control (ANOVA). (B) An overlay of the curves of distribution of CD11b mean cell fluorescence intensity is shown for control (hatched) and stressed groups (solid grey) at D1 as well as a representative dot-plot showing gated F4/80+/CD11b + cells in control and stressed groups(C). (*D*) *Overlay of the distribution of unstained cells (grey) and APC-F4/80 stained cells (hatched) from a representative experiment gated for F4/80 positive cells. The auto-fluorescence represents less than 0.5% of the histogram.*

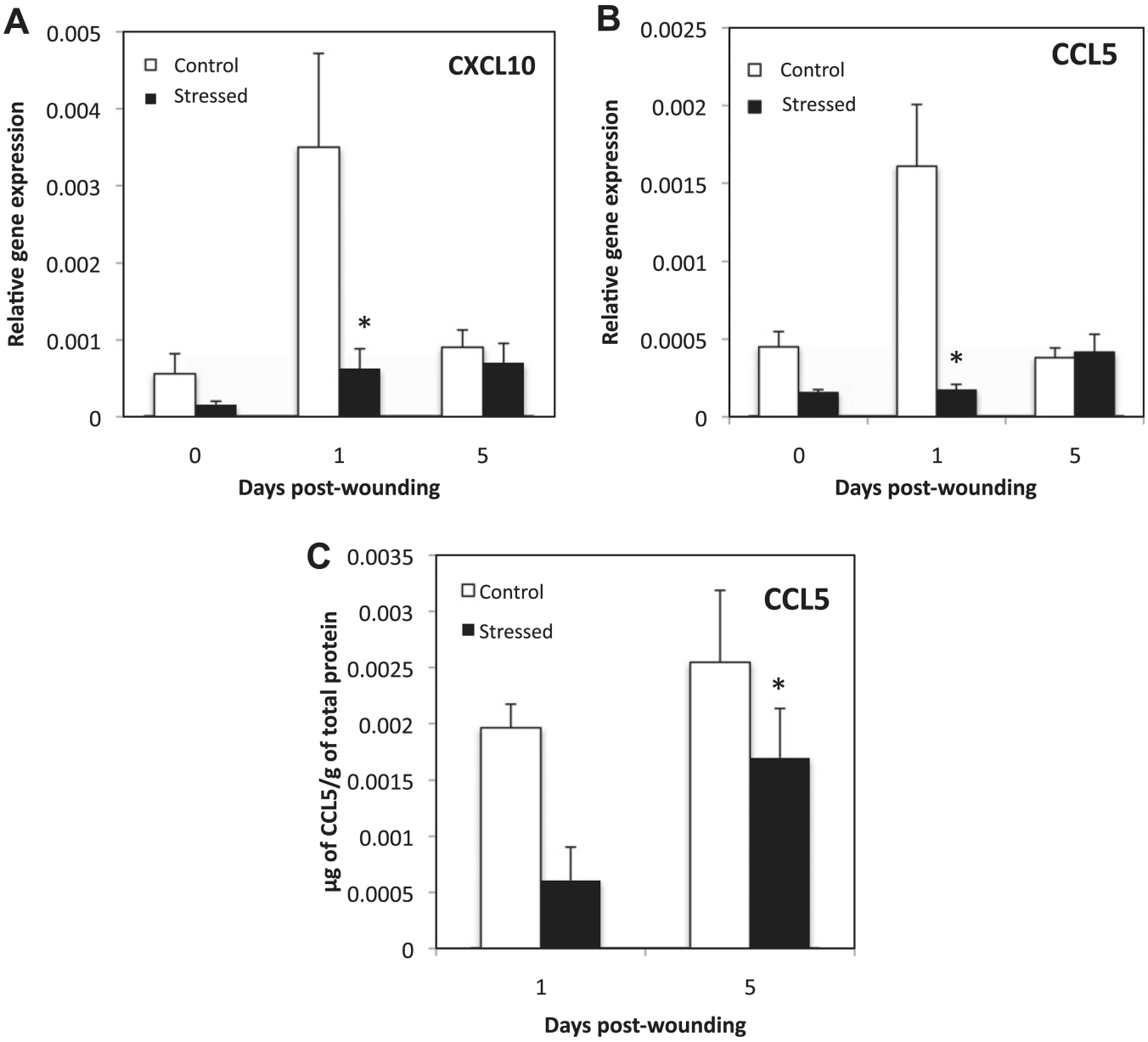

Fig. 7.

Markers of classically activated macrophages. Unwounded skin and wounds were harvested at 1 and 5 days post-wounding. Gene expression of CXCL10 (A), and CCL5 (B) was measured and normalized to the housekeeping gene GAPDH using qRT–PCR. Data represent mean ± SEM from 4 experiments. At each time point $n = 20$ mice/group. (C) Represents the protein concentration of CCL5 in µg/g of total protein from tissue extract of Day 5 wounds from control and stressed mice. Data represent mean ± SEM from $n = 3$–4 mice/group. $^{*}p \leq 0.05$ Compared to control.

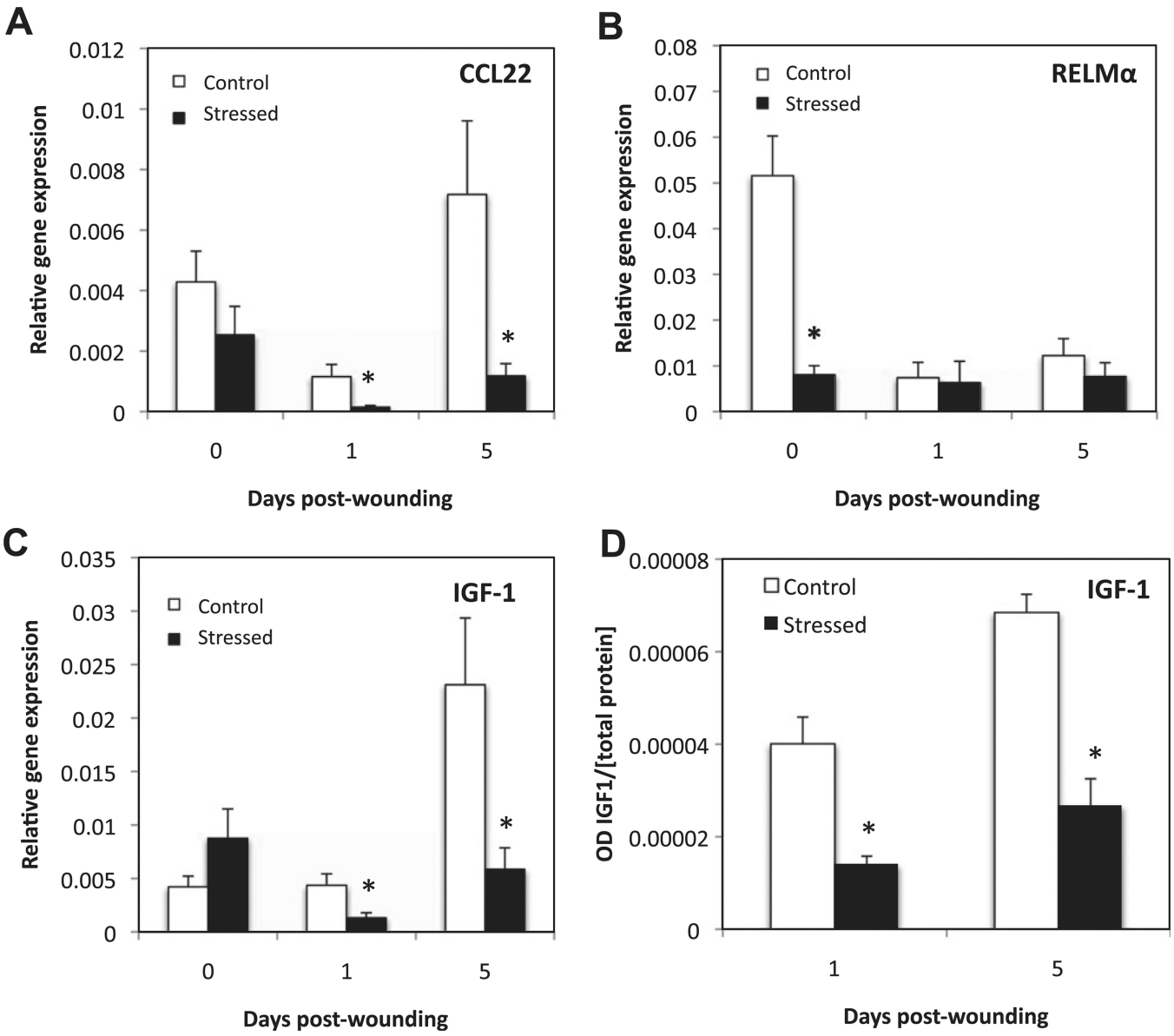

Fig. 8.

Markers of wound-healing macrophages. Unwounded skin and wounds were harvested at 1 and 5 days post-wounding. Gene expression of CCL22 (A), RELMα (B), and IGF-1 (C) was measured and normalized to the housekeeping gene GAPDH using qRT-PCR. Data represent mean ± SEM from 4 experiments. At each time point n = 20 mice/ group. (D) Represents the OD for IGF-1 per μg of total protein from tissue extract of Day 1 and 5 wounds of control and stressed mice. Data represent mean ± SEM from n = 4 mice/ group. $^{*}p < 0.05$ Compared to control (ANOVA).

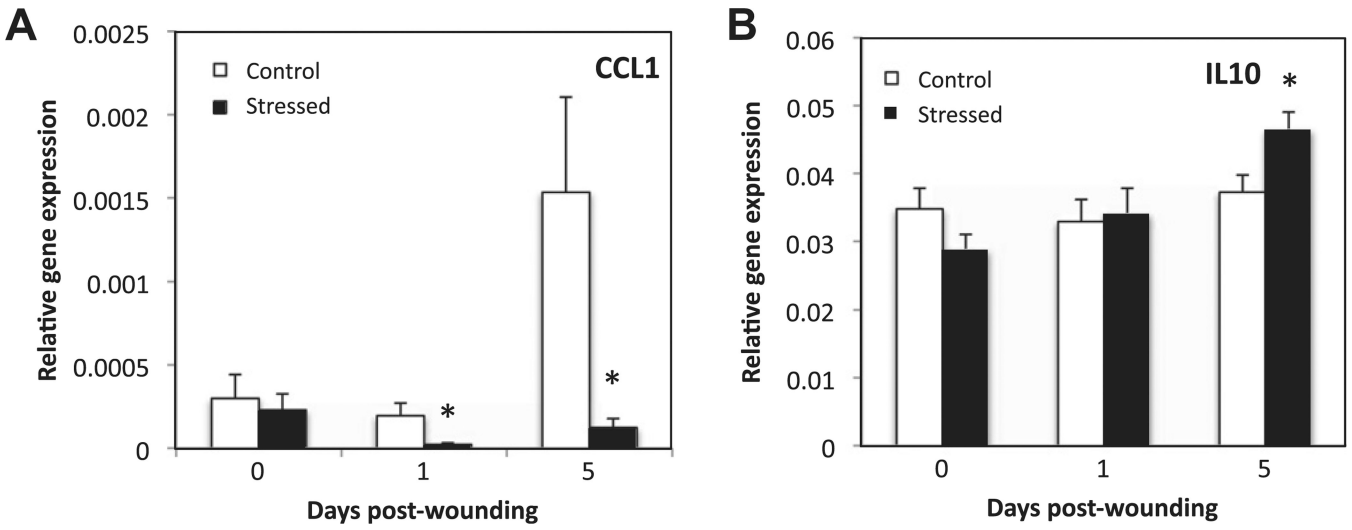

Fig. 9.

Markers of regulatory macrophages. Unwounded skin and wounds were harvested at 1 and 5 days post-wounding. Gene expression of CCL1 (A) and IL10 (B) was measured and normalized to the housekeeping gene GAPDH using qRT–PCR. Data represent mean ± SEM from 4 experiments. At each time point $n = 20$ mice/group. $^{*}p \leq 0.05$ Compared to control (ANOVA).

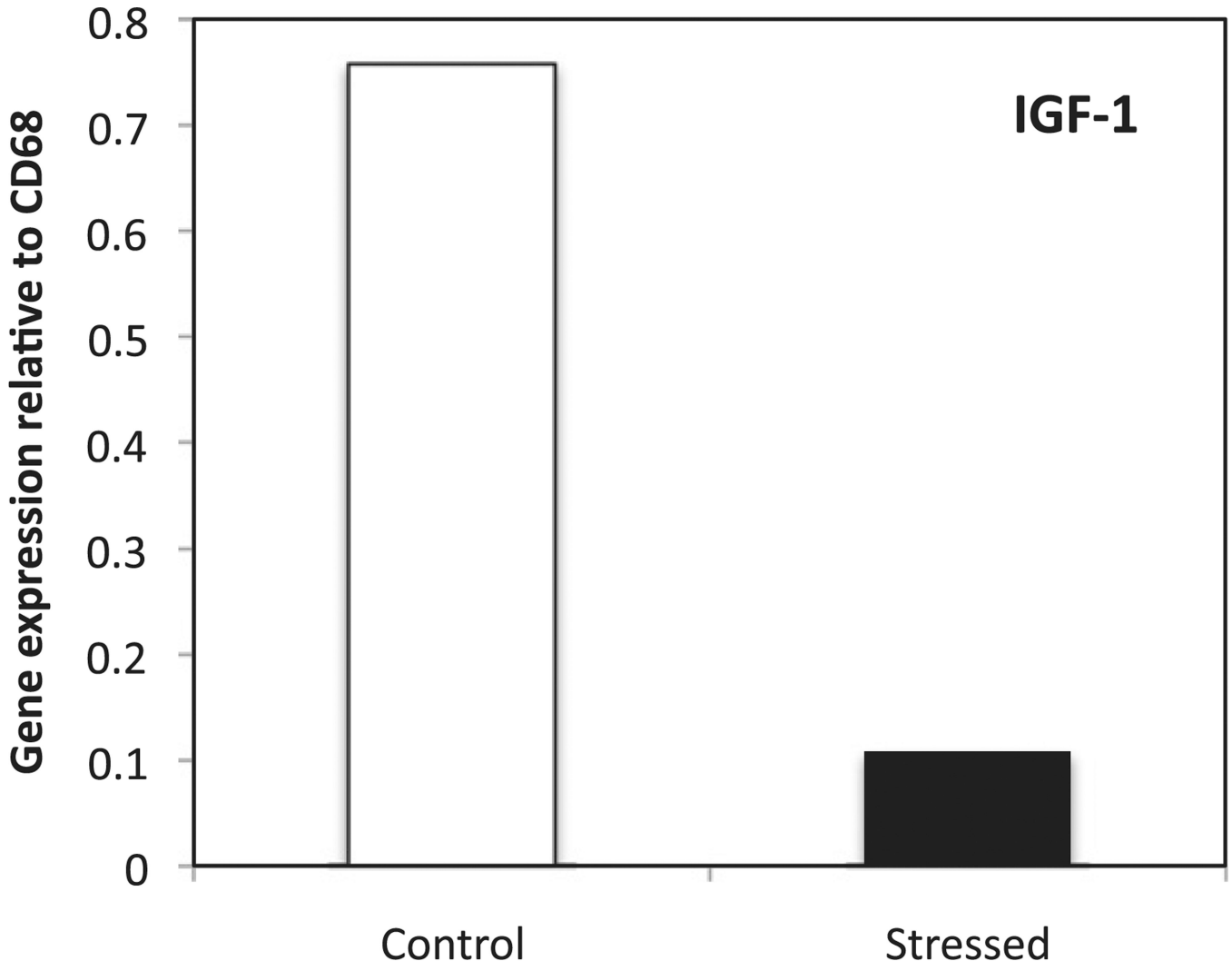

Fig. 10.

Gene expression of IGF-1 in macrophages isolated by LCM. Tissue sections of wounds from control and stressed mice at D5 were stained against CD68. Macrophages were microdissected using LCM and qRT–PCR was performed. Data represent mean from approximately 4000 cells/sample.